

## Article

# Seismic Performance Screening and Evaluation for Embankments on Liquefiable Foundation Soils

Chih-Chieh Lu <sup>1,\*</sup>, Kuan-Yu Chen <sup>1</sup>, Yun-Ta Cheng <sup>2</sup> and Yu-Hung Han <sup>2</sup><sup>1</sup> National Center for Research on Earthquake Engineering, Taipei 106219, Taiwan; kyc@narlabs.org.tw<sup>2</sup> Water Resources Planning Institute, Water Resources Agency, Ministry of Economic Affairs, Taichung 413001, Taiwan; ytcheng@wrap.gov.tw (Y.-T.C.); newb025040002@gmail.com (Y.-H.H.)

\* Correspondence: chchlu@narlabs.org.tw

**Abstract:** This paper proposes a framework for screening and evaluating seismic performance of river earth embankments on liquefiable foundation soils. The framework is executed in the order of simplest screening by soil liquefaction potential map to preliminary and detailed evaluation of seismic performance of embankment according to the sufficiency of data and the complexity and accuracy of the methods. The seismic performances of embankments are classified into four levels based on the seismic-induced crest settlement. The method used for preliminary evaluation is based only on the factors of safety of foundation soils against liquefaction and the embankment slope against sliding. The static softening method (SSM) and dynamic effective stress method (DESM) are suggested for detailed evaluation of seismic performance. SSM is a static FDM or FEM analysis for estimating liquefaction-induced settlement by weakening the strength of the liquefied foundation soil under the action of the self-weight of the embankment. However, DESM is a dynamic history analysis for estimating liquefaction-induced settlement by simulating the generation and dissipation of pore water pressure in the liquefaction process of foundation soils under the action of the self-weight of the soil embankment and its seismic inertial force. The damaged embankment of the Maoluo River in the 1999 Chi-Chi earthquake was used as a case to demonstrate the feasibility of this framework. The results showed that the simpler the adopted method is, the more conservative the estimated settlement.

**Keywords:** embankment; soil liquefaction; seismic performance

**Citation:** Lu, C.-C.; Chen, K.-Y.; Cheng, Y.-T.; Han, Y.-H. Seismic Performance Screening and Evaluation for Embankments on Liquefiable Foundation Soils. *Geosciences* **2022**, *12*, 221. <https://doi.org/10.3390/geosciences12060221>

Academic Editors: Francesca Bozzoni, Claudia Meisina and Jesus Martinez-Frias

Received: 6 April 2022

Accepted: 20 May 2022

Published: 24 May 2022

**Publisher's Note:** MDPI stays neutral with regard to jurisdictional claims in published maps and institutional affiliations.



**Copyright:** © 2022 by the authors. Licensee MDPI, Basel, Switzerland. This article is an open access article distributed under the terms and conditions of the Creative Commons Attribution (CC BY) license (<https://creativecommons.org/licenses/by/4.0/>).

## 1. Introduction

As an important water conservancy facility to prevent flooding, river embankments are rarely designed to consider their seismic performances, and due to the limitation of project cost, river embankments are mostly made of existing riverbed materials and simply piled up, making the construction quality of the embankments less reliable. Therefore, the seismic performance of the river embankment is usually poor and is easily damaged under the shaking of strong earthquakes. There are many actual case histories of embankments that were damaged by strong earthquakes, such as the 1995 Kobe Earthquake, the 2011 Great East Japan Earthquake, and 2018 Hokkaido Earthquake in Japan [1–3], the 2012 Emilia Earthquake in Italy [4], and the 1999 Chichi Earthquake and the 2016 Meinong Earthquake in Taiwan [1,5]. Among the damaged embankments of the case histories, there are many large-scale deformation cases, where the crest settlements of the damaged embankments exceeded 3 m. Many of them are located in the old river channels and estuary alluvial fans where soil liquefaction easily occurs. Therefore, after the earthquake, it was found that many embankments were seriously damaged due to soil liquefaction. Based on the summary report of the River Embankment Earthquake-Resistant Measures Emergency Review Committee [2], in addition to the damages caused by liquefaction of foundation ground, much damage was caused by the liquefaction of the embankment body, and

this also requires special attention. During strong earthquakes, when the foundation and embankment soils liquefy, the soils may lose much of their moduli and strengths and be unable to support their overlying embankment weights. The above damage mechanism of embankments due to liquefaction is shown in Figure 1. Lessons learned from the 1995 Kobe Earthquake, the 1999 Chichi Earthquake, and the 2011 Great East Japan Earthquake showed that it is difficult to restore damaged embankments during the period from the earthquake to the flood season and rainy season that follows, due to the excess of damaged sections and their extensive distributions. It is also worthy to notice that the moment magnitudes of the 2012 Emilia Earthquake, the 2016 Meinong Earthquake, and the 2018 Hokkaido Earthquake were just 6.1, 6.4, and 6.6, respectively. These events demonstrate that the earthquakes of moderate magnitude can cause serious damages of river embankments.

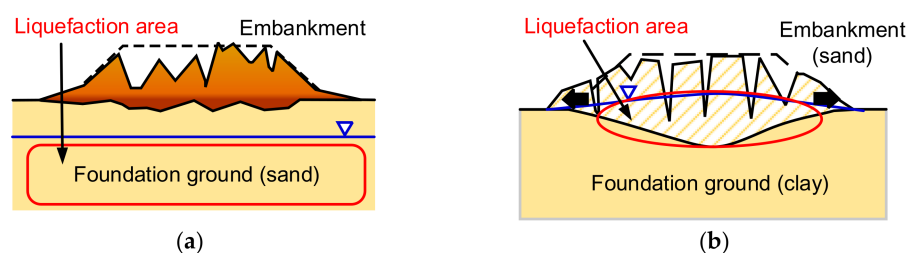


**Figure 1.** Damage mechanism of embankments due to liquefaction; (a) liquefaction occurring in foundation, (b) liquefaction occurring in embankment.

The above-mentioned earthquake damage cases for river embankments show that the seismic safety of river embankments is a geo-earthquake engineering issue that must be faced by geotechnical engineers. Some researchers have expended much effort on the seismic evaluation of embankments. Over the last sixty years, the framework of seismic performance evaluation for embankment dams has been well-developed. However, the seismic safety of river embankments draws far less attention than earth dams due to their differing importance. In essence, the seismic evaluation approaches used in embankment dams can be also applied to river embankments. In the past, many researchers have made contributions to this area. For example, Kramer [6] suggested three steps to evaluate the seismic performance of an embankment located on a liquefiable deposit as follows: (1) assessment of liquefaction susceptibility; (2) triggering of liquefaction; and (3) post-liquefaction stability analysis (i.e., consequence of flow slide). The procedure is generally adopted in practice. Athanasopoulos-Zekkos and Saddi [7] proposed guidelines for selecting ground motions for liquefaction evaluation analysis of earth levees. Perlea et al. [8] summarized the procedures for seismic evaluation of levees and suggested that the selected evaluation methods should be based on the available data of river embankments. In most cases, the soil data is insufficient to justify the use of sophisticated procedures such as FEM/FDM dynamic time history analysis. Athanasopoulos-Zekkos and Seed [9] developed a simplified methodology for consideration of the 2D dynamic response of levees in a liquefaction-triggering evaluation. Okamura and Hayashi [10] used a centrifuge model test, while Athanasopoulos-Zekkos et al. [11] have proposed guidelines for selecting ground motions for evaluation of seismic slope displacements for earthen levees. Gobbi et al. [12] used OpenSees to analyze the soil-liquefaction-induced failure of embankments. Chiaradonna et al. [13] proposed a calibration procedure to derive parameters for a pore water pressure generation model using SPT and CPT. Chiaradonna et al. [14] suggested a parameter calibration framework of PM4Sand model using the results of triaxial testing, simple shear testing, and centrifuge model testing to better simulate the seismic response of an embankment.

However, guidelines for regulating the earthquake-resistant safety of river embankments are rare. In Japan, a country with active earthquakes, increased attention began to be given to the earthquake-resistant performance of river embankments after the 1995 Kobe Earthquake, which caused extensive damage to river embankments. In 2011, the



Water and Disaster Management Bureau of the Ministry of Land, Infrastructure, Transport and Tourism [15] issued standard procedures for earthquake resistance inspection and evaluation of river embankments. The process mainly includes three stages of earthquake resistance assessment, from the simplest and rough inspection to the most complex and detailed three inspections. The corresponding data collection and investigation also increase, and the evaluation method is also more complex. The process proposed by the Ministry of Land, Infrastructure, Transport and Tourism of Japan can effectively identify important river embankments with insufficient seismic safety in stages and carry out seismic reinforcement to avoid the secondary disaster of flooding after the earthquake. Therefore, it is more cost-effective and reasonable to allocate resources. It is a work process worthy of reference. In Canada, the Ministry of Forests, Lands, and Natural Resource Operations—Flood Safety Section (2011) also started planning earthquake-resistant design guidelines for river embankments, which were published in 2014 [16,17]. The contents of the report are quite complete and worth reference, covering earthquake risk and analysis, water outlet height, geotechnical investigation, performance design, analysis method, reinforcement strategy, and post-earthquake inspection.

In Taiwan, although there have been many cases of river embankments damaged by past earthquakes, such as the 1999 Chichi Earthquake and the 2016 Meinong Earthquake, there are no domestic regulations for the inspection and seismic assessment of river embankments. However, the river embankments located in liquefaction potential areas are an issue that needs more attention. Figure 2 shows the overlapping results of the distribution of river embankments and soil liquefaction potential map in the Taipei Basin. As shown in the figure, many river embankments, which guard the safety of New Taipei City, are located in areas with high liquefaction potential and require special attention. The first goal of this study is to refer to the experience of other countries in implementing seismic safety assessments on embankments. The second purpose of this study is to propose a process for the seismic assessment of river embankments suitable for Taiwan's local characteristics and demonstrate the analyses with a real case, so as to facilitate the reference application of relevant government units for seismic performance evaluation of critical embankments.

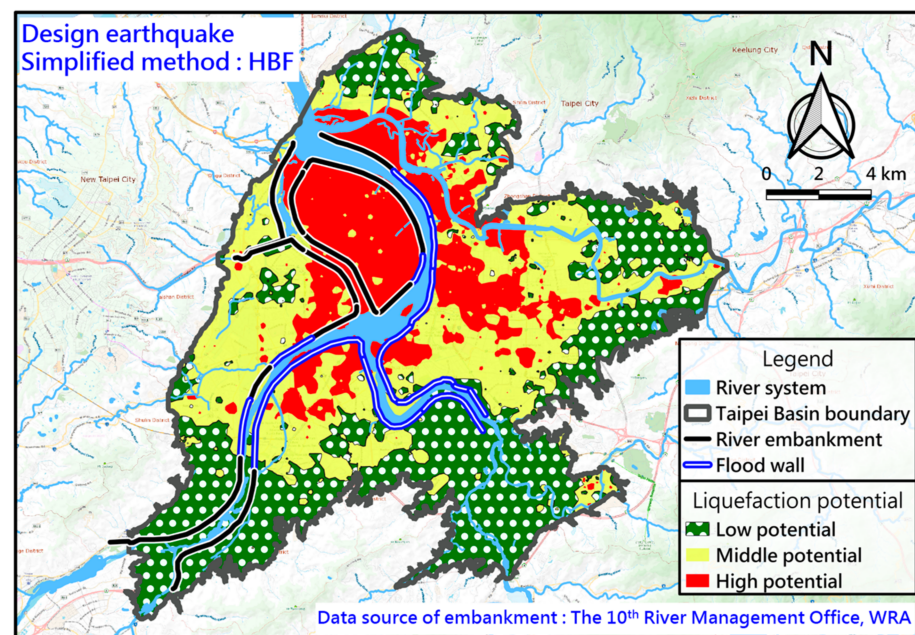


**Figure 2.** The distribution of river embankments and liquefaction potential in the Taipei Basin.

## 2. The Consideration for the Seismic Assessment

### 2.1. Seismic Performance

In order to avoid flooding after a strong earthquake, river embankments have to meet two conditions. One is that the elevation of the embankment must be higher than the flood elevation to avoid flood overflow, and the other is that the river embankment itself has the function to avoid the scouring or piping of the flood. After a large earthquake, strong ground shaking can easily cause the river embankment and its underlying foundation to settle, loosen, and crack, and compromise the function of flood prevention. Nonetheless, an earthquake-damaged river embankment should still ensure short-term flood prevention function, so that the stakeholder has enough time to complete repair work before flood onset. Due to the wide distribution of river embankments, it is necessary to identify the river embankments that cannot provide short-term flood control functions after the earthquake, and plan and strengthen them to avoid secondary disasters caused by heavy rainfall after the earthquake.

This study adopted the post-seismic height of the embankment as the performance requirement. The considered earthquake was the design earthquake (return period of 475 years) in national codes. The recommended return period of the flood considered for post-earthquake repair is 2 years. The allowable settlement of the embankment crest after the earthquake is the difference between the embankment crest elevation and the considered flood level during the repair period. It should be noted that the consideration of the flood level during the post-earthquake repair period can also be adjusted according to the needs of the stakeholders. If the considered flood level outside the embankment is higher (the return period is longer, and the probability of occurrence is low), and the allowable settlement of the embankment top after the earthquake is smaller, it means that the allowable repair time for the damaged river embankment is longer. Conversely, if the considered flood level outside the embankment after the earthquake is lower (the return period is shorter and the probability of occurrence is high), and the allowable settlement of the top of the embankment becomes larger after the earthquake, the repairable time for the damaged embankment is shorter.

### 2.2. Seismic Safety Classification

Following the seismic performance parameters addressed in the previous section for the seismic safety classification of river embankments, this study focused on two damage scenarios; namely, the damage degree of the embankment and the flood overflow, using the more conservative scenarios as the basis for the seismic safety classification. Table 1 shows the seismic safety classification and performance requirements of river embankments. The seismic safety level ranges from high to low, and is divided into I, II, III, and IV. The boundary of each seismic safety level is 25%, 50%, and 75% of the embankment height. If the settlement of the embankment is greater than the allowable settlement, it is directly classified as the worst grade, IV.

**Table 1.** Seismic safety classification of an embankment.

Classification	Post-Seismic Settlement of Embankment Crest	
	Damage Degree of the Embankment	Flood Overflow
I	<25% of the embankment height	-
II	25~50% of the embankment height	-
III	50~75% of the embankment height	-
IV	>75% of the embankment height	>the allowable settlement

### 2.3. Seismic Assessment Process for River Embankments

River embankments are widely distributed on both sides of major and minor rivers, the management of which need ample effort and resources. Therefore, when planning the

seismic safety assessment process, it is advisable to use simple methods as much as possible to first screen out the ones with a lower risk of damage in order to efficiently proceed with seismic assessment work. According to past experience, the main cause of serious damage to river embankments is earthquake-induced soil liquefaction; earthquake shaking alone rarely causes large-scale sliding and collapse damage of river embankments. Therefore, the research first excluded river banks without soil liquefaction concerns, and focused on river embankments with soil liquefaction damage potential.

This study refers to the relevant standard procedures for seismic inspection and assessment of river embankments proposed in Japan, and attempts to simplify the procedure in order to consider the situation in Taiwan. Figure 3 is the seismic safety classification process of river embankments proposed in this study. In this work, the basic data required for seismic evaluation was collected first, including the geometric and material properties of the river embankment, geological data, design flood elevation, seismic hazard characteristics, and the liquefaction potential of the site, etc. After that, simple screening criteria according to the soil liquefaction potential maps (e.g., Figure 2), micro-topography, and historical earthquake disaster cases were used to exclude low liquefaction risk embankments. If an embankment had a risk of soil liquefaction, a preliminary seismic evaluation based on the formula calculation was carried out to classify the embankment according to Table 1. River embankments belonging to Class I did not need further detailed seismic evaluation. If the river embankment belonged to other classes, detailed seismic evaluation was carried out to obtain a more reasonable seismic response from the embankment. When conducting a detailed seismic assessment, supplementary surveys may need to be carried out to obtain the parameters required for the analysis. The detailed seismic evaluation can be conducted by static softening method (SSM) or dynamic effective stress method (DESM). Both of them should be carried out by means of finite element or finite difference programs. The preliminary and detailed seismic evaluation are introduced in following section.

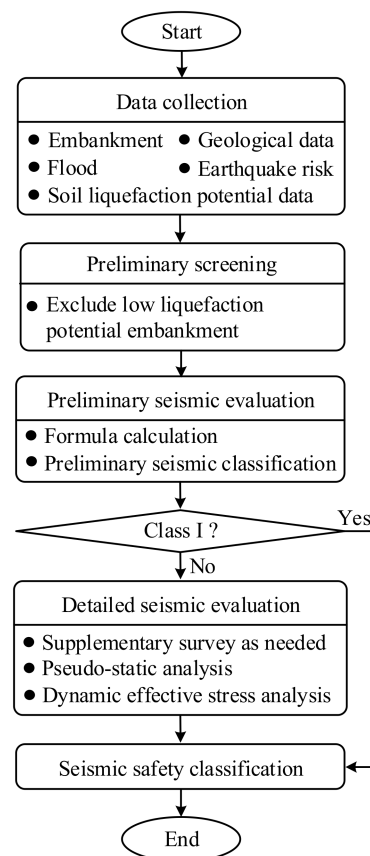


**Figure 3.** Seismic classification process of river embankments.

### 3. Seismic Evaluation of the Embankments

#### 3.1. Preliminary Seismic Evaluation

In April 2007, the “Coastal Conservation Facility Seismic Inspection Manual” jointly issued by the Japanese Ministry of Agriculture, Forestry and Fisheries, the Ministry of Transport, and the Ministry of Construction proposed a simple method to evaluate the safety of river embankments subjected to seismic force and soil liquefaction. It is believed that it can be applied to the earthquake resistance assessment of river embankments in Taiwan. The method is slightly modified according to the Taiwanese condition and introduced as follows:

The analysis needs to collect the information of the geometry and materials of the embankment and the foundation soils, and then calculate the static factor of safety ( $F_{S0}$ ) using Equation (1). The factor of safety in the equation is obtained from traditional limit equilibrium analysis. Note that the foundation soils should be simplified to a single soil layer if the ground consists of multi-layers soils. Sensitive study may be needed if the ground formation is complex.

$$F_{S0} = \mu_1 \mu_2 F_{SS} \tag{1}$$

where  $\mu_1$  is the correction coefficient considering the ratio of the depth of foundation ground to the height of embankment, which is 1.0 for sandy ground and should be derived from Figure 4 for clayey ground;  $\mu_2$  is the correction coefficient considering the horizontal length in front of the embankment toe, which can be derived from Table 2;  $F_{SS}$  is the standard factor of safety, which is  $N_1 \tan(\phi)$  for sandy soils and  $N_2 c$  for clay soils; and  $c$  and  $\phi$  are cohesion and friction angle of soils, respectively.  $N_1$  and  $N_2$  are the soil type dependent coefficients, which should be derived from Figure 5.

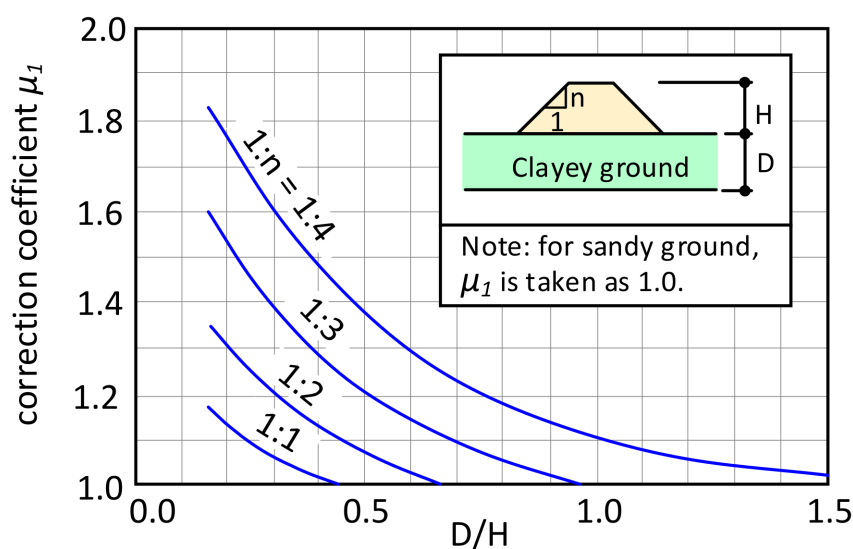


Figure 4. The relationship between the correction coefficient ( $\mu_1$ ) and  $D/H$ .

Table 2. Correction coefficient  $\mu_2$  for the influence of horizontal length in front of the embankment toe.

Horizontal Length in Front of the Embankment toe $\ell$ (m)	Correction Coefficient $\mu_2$
$\ell \leq 10$	0.8
$10 < \ell \leq 30$	0.9
$30 < \ell$	1.0

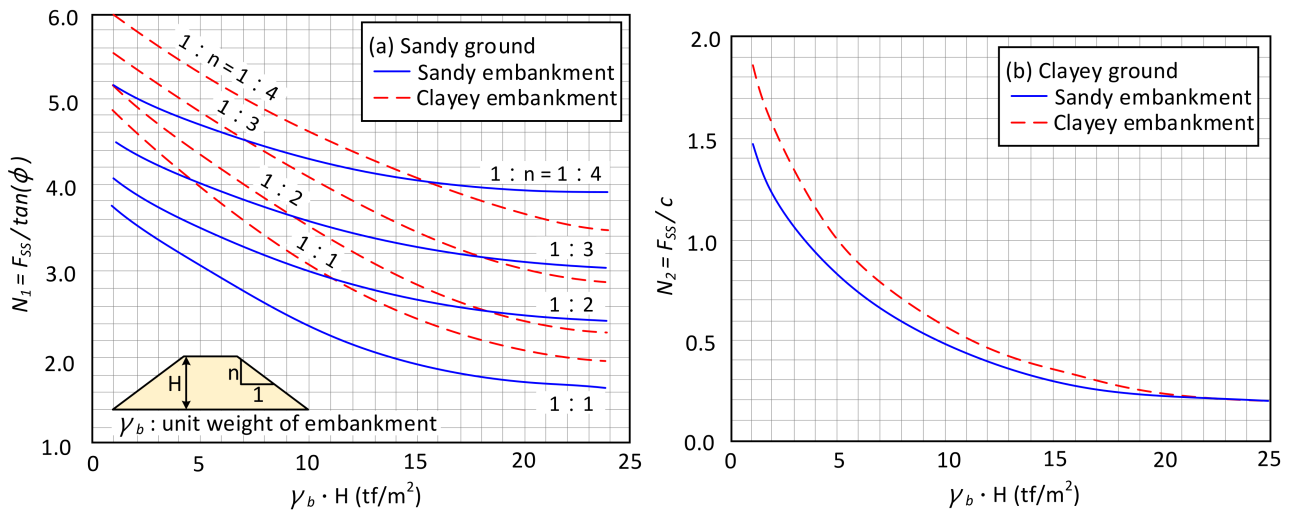


Figure 5. Soil-type-dependent coefficients. (a) sandy ground; (b) clayey ground.

After the calculation of the static factor of safety ( $F_{S0}$ ), the dynamic factor of safety ( $F_{Sd}$ ) was calculated next. The dynamic factor of safety was calculated by considering two scenarios of earthquake-induced inertial force  $F_{Sd}(k_h)$  and soil liquefaction  $F_{Sd}(\Delta u)$  independently. The calculation of  $F_{Sd}(k_h)$  is shown as follows.

$$F_{Sd}(k_h) = \alpha \cdot F_{S0} \tag{2}$$

where the  $\alpha$  is the reduction factor considering the action of earthquake-induced inertial force and should be derived from Figure 6. Note that the horizontal seismic coefficient  $k_h$  in the figure is equal to one-half of peak ground acceleration (PGA).

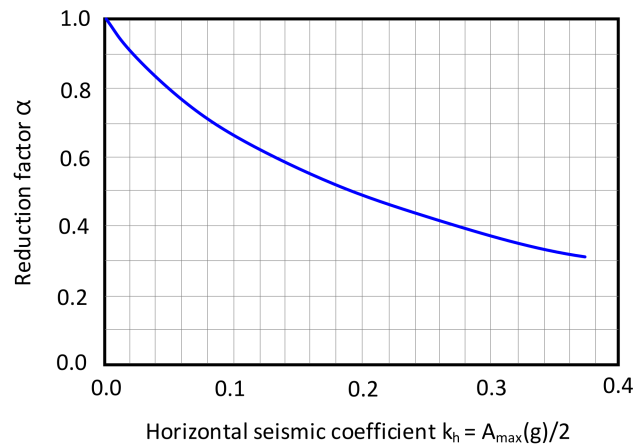


Figure 6. The relationship between reduction factor  $\alpha$  and horizontal seismic coefficient  $k_h$ .

The calculation of  $F_{Sd}(\Delta u)$  is shown as follows.

$$F_{Sd}(\Delta u) = \beta \cdot F_{S0} \tag{3}$$

where the  $\beta$  is the reduction factor considering the occurrence of soil liquefaction, which can be obtained from Table 3.



**Table 3.** Reduction factor  $\beta$  for soil liquefaction to the static factor of safety.

Factor of Safety against Soil Liquefaction ( $F_L$ ) <sup>a</sup>	Reduction Factor $\beta$	
	Condition A <sup>b</sup>	Condition B <sup>c</sup>
$F_L \leq 1.0$	0.25	0.4
$1.0 < F_L \leq 1.1$	0.45	0.6
$1.1 < F_L \leq 1.25$	0.7	0.85
$1.25 < F_L \leq 1.5$	0.9	0.95
$1.5 < F_L$	1.0	1.0

<sup>a</sup> The  $F_L$  of each layer of the ground should be derived according to the stress-based simplified method. The minimum  $F_L$  is used to evaluate  $\beta$ . <sup>b</sup> Condition A: the minimum  $F_{S0}$  occurs when simplified model of multi-layer ground is sandy material. <sup>c</sup> Condition B: the minimum  $F_{S0}$  occurs when simplified model of multi-layer ground is clayey material.

Upon obtaining  $F_{Sd}(k_h)$  and  $F_{Sd}(\Delta u)$ , the seismic safety classification and the settlement prediction of an embankment can be evaluated according to Table 4. Note that the conservative results of the two criteria in the table should be chosen for the conservative bias principle of the preliminary seismic evaluation.

**Table 4.** Evaluation of seismic capacity of a river embankment based on  $F_{Sd}$ .

Classification	Damage Degree of the Embankment	Dynamic Factor of Safety ( $F_{Sd}$ )	
		$F_{Sd}(k_h)$	$F_{Sd}(\Delta u)$
I	<25% of the embankment height	$1.0 < F_{Sd}$	
II	25%~50% of the embankment height	$0.8 < F_{Sd} \leq 1.0$	
III	50%~75% of the embankment height	$F_{Sd} \leq 0.8$	$0.6 < F_{Sd} \leq 0.8$
IV	>75% of the embankment height	-	$F_{Sd} \leq 0.6$

3.2. Detailed Seismic Evaluation (Static Softening Method, SSM)

The static softening method (SSM) is one of the suggested detailed seismic evaluation methods for a river embankment and relies on finite elements or finite difference numerical programs to simulate the deformation of the embankment and the foundation stratum after earthquake. In comparison with the dynamic effective stress method (DESM), the SSM is a relatively simple analysis that can consider the self-weight deformation of the river embankment caused by the effect of soil liquefaction. The concept of the method is shown in Figure 7.

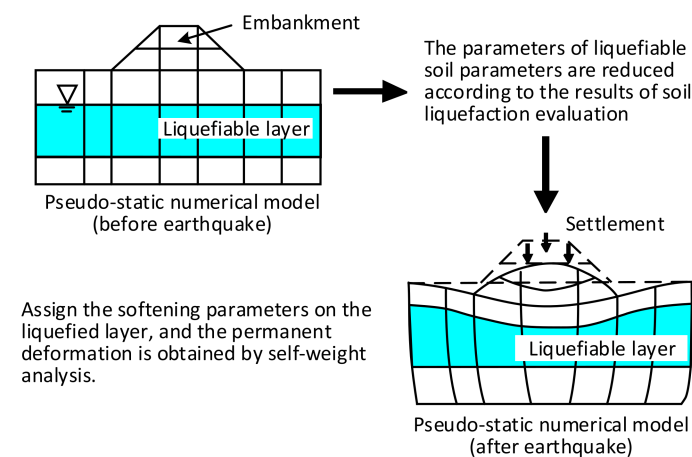


**Figure 7.** The concept of the static softening method (SSM).

Before conducting the numerical analysis, it was necessary to collect the drilling data of the site and the information of the design earthquake and then conduct the stress-based simplified procedure such as the methods of HBF [18], NCEER [19], JRA [20], and AIJ [21] to identify the liquefaction potential stratum. Upon obtaining the above information, a numerical model of the river embankment was carried out to obtain the pre-seismic deformation. After that, the strength and stiffness of the soils with  $F_L < 1.0$  based on the soil liquefaction evaluation was modified to simulate the mechanical behavior of liquefaction. To the strength of the liquefied soils, the residual shear strength was assigned according to Stark and Mesri [22] and Idriss and Boulanger [23], who established the relationship between normalized residual shear strength ( $S_u/\sigma'_{v0}$ ) and clean sand equivalence of corrected SPT blow count ( $(N_1)_{60cs}$ ) shown in Figure 8 and the formula are summarized in Equations (4)–(7) as follows.

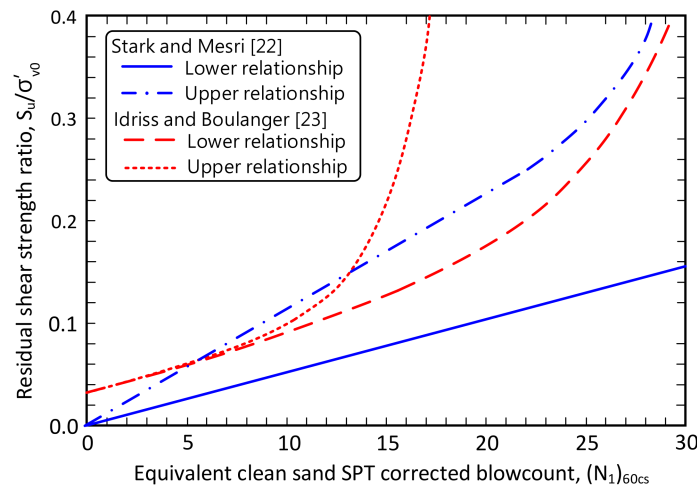


**Figure 8.** The relationship between normalized undrained residual shear strength  $S_u/\sigma'_{v0}$  and clean sand equivalence of corrected SPT blow count ( $(N_1)_{60cs}$ ).

Upper relationship suggested by Stark and Mesri [22]

$$S_u/\sigma'_{v0} = 0.011 \times (N_1)_{60cs} \text{ for } (N_1)_{60cs} < 20 \tag{4}$$

Lower relationship suggested by Stark and Mesri [22]

$$S_u/\sigma'_{v0} = 0.0055 \times (N_1)_{60cs} \tag{5}$$

Upper relationship suggested by Idriss and Boulanger [23]

$$S_u/\sigma'_{v0} = \exp\left(\frac{(N_1)_{60cs}}{16} + \left(\frac{(N_1)_{60cs} - 16}{21.2}\right)^3 - 3.0\right) \times \left(1 + \exp\left(\frac{(N_1)_{60cs}}{2.4} - 6.6\right)\right) \tag{6}$$

Lower relationship suggested by Idriss and Boulanger [23]

$$S_u/\sigma'_{v0} = \exp\left(\frac{(N_1)_{60cs}}{16} + \left(\frac{(N_1)_{60cs} - 16}{21.2}\right)^3 - 3.0\right) \tag{7}$$

Upon identifying the residual strength of the liquefied soils, the Young’s modulus (E) could be obtained based on the empirical ratio of the Young’s modulus to the residual strength ( $E/S_u = 300$ ). Because the liquefied soil tends to undrained condition, the Poisson’s ratio ( $\nu$ ) of 0.49 is assumed. The shear modulus and bulk modulus could be also obtained using the E and  $\nu$  according to the theory of elasticity.

After replacing the parameters of the soils with  $F_L < 1.0$ , the post-earthquake deformation analysis was carried out; then, the post-earthquake river embankment deformation was deduced from that of before the earthquake.

### 3.3. Detailed Seismic Evaluation (Dynamic Effective Stress Method, DESM)

The dynamic effective stress method (DESM) for analyzing a river embankment is the most complete and complex analysis method using finite element or finite difference numerical programs. The DESM first discretizes the entire earthquake in the time domain, and then calculates each discrete time point step by step with the complicated soil constitutive models in order to obtain the response of the entire numerical analysis model in the time duration. The calculation of DESM is time-consuming, and the analysis theory and the determination of the input motion duration of the representative base are complicated, so that its practical application is not as good as that of SSM. However, since the SSM ignores the time factor, the inertial force and damping effect of the soil cannot be considered. Therefore, it is still recommended to conduct DESM in the river embankment section with high importance and great secondary disaster impact.

The analysis concept of DESM is shown in Figure 9. This method needs to establish the numerical model and directly inputs the dynamic loading at the bottom boundary. The dynamic responses of the embankment can be automatically simulated by the numerical program through its assigned constitutive model. When performing DESM, the soil elements need to reasonably reflect the dynamic characteristics, including the hysteretic damping, modulus degradation properties, and generation of excess pore water pressure. Therefore, the commonly used Mohr–Coulomb model is insufficient. In this regard, the stress–strain response of Masing’s rule is suggested to be used for clay or gravel, which have low liquefaction potential and for which the amount of water pressure generation is little. In contrast, for saturated sandy soils that may liquefy, it is recommended to use soil constitutive modes that can further consider the generation of excess pore water pressure during the cyclic loading, such as the Finn model [24] or PM4Sand model [25].

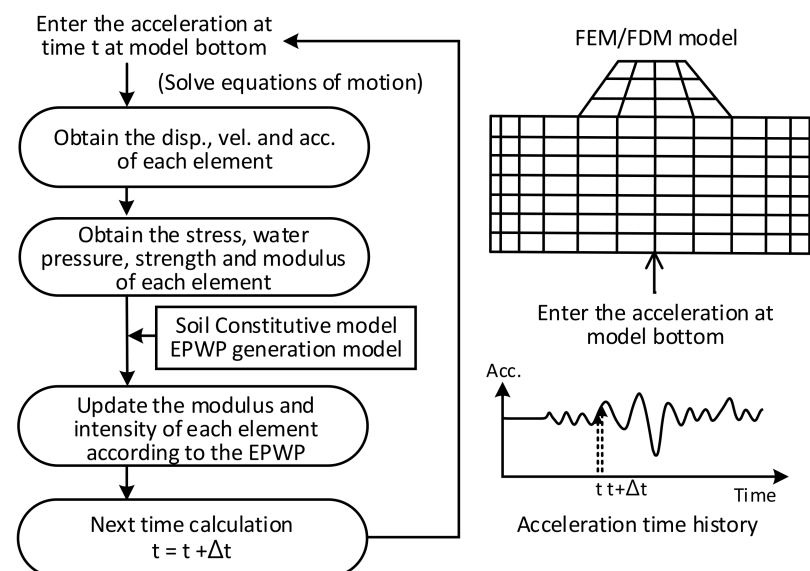


**Figure 9.** The concept of the dynamic effective stress method (DESM).

The selection of the representative earthquake, which means the input motion for the numerical model, is another important issue for the DESM. Earthquakes are affected by different geological conditions and source characteristics. Therefore, the characteristics of the site need to be considered when selecting the design earthquake. Generally, the acceleration amplitude and design response spectrum of the site should be first derived according to the national seismic design code. Then the seismic records of a typical earth-

quake monitored by the seismic station closest to the site can be used as a seed earthquake. Since the embankment is a plane strain structure, the EW and NS components of the seed earthquake should be transferred to the controlled direction, which is perpendicular to the alignment of the embankment. The acceleration history is then filtered by low-pass-filter in order to eliminate high frequency signals. After, spectral matching in the frequency domain is carried out based on response design spectrum and the seed earthquake after the adjustment of the action direction to obtain an acceleration time history appropriate to the site conditions. Note that in order to meet the response spectrum of the design earthquake, the waveform of the seed earthquake was artificially modified. Because the considered earthquake is an outcrop motion, to be the input motion at the bottom boundary of the numerical model, which is within condition, the acceleration amplitude of the considered earthquake should be divided by two. Note that some computer codes can automatically perform deconvolution to derive the input motions at the input base when declaring that the input motion used is an outcrop-type motion. The way to determine the input motion in this study is straightforward but a little conservative owing to not considering the downward wave into the underlying half space. The complete procedure to yield the input motion is shown in Figure 10.

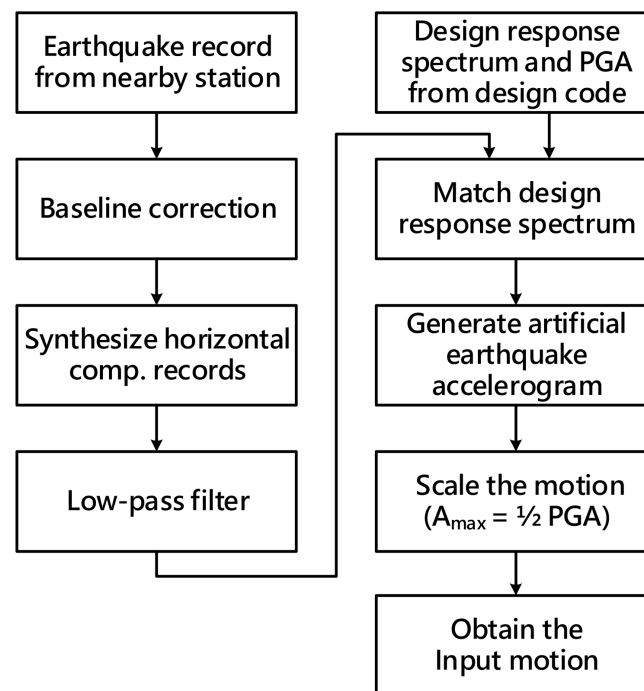


Figure 10. The procedure to determine the input motion.

#### 4. Case Study

This study selected the river embankment next to Maoluo River in Nantou City as a calculation example. The location of the demonstration site as well as the seismic station and active fault of this study is shown in Figure 11. The river embankment section suffered significant settlement during the 1999 Chi-Chi Earthquake, as shown in Figure 12. Due to the earthquake damage investigation and restoration in this area after the earthquake, the relevant information can be found in the literature, which is suitable for a demonstration case. This study collected the relevant river bank data, design earthquake, and drilling data, and then conducted a preliminary and detailed seismic evaluation of the river embankment.

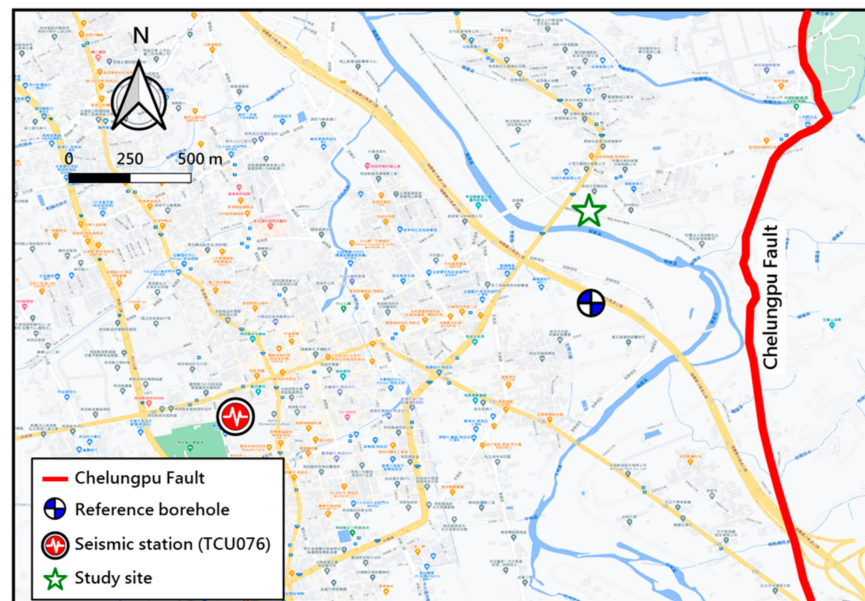


Figure 11. The location of the demonstration site.



(a)

(b)

Figure 12. Damage of the demonstration site after 1999 Chi-Chi Earthquake, (a) settlement of the embankment, (b) lateral spread of floodplain.

#### 4.1. Basic Data of the Demonstration Site

The river embankment next to the Nantou Jungong Bridge (Baowei revetment) was used as a demonstration case for analysis. The geometry of the river embankment is based on the actual measurement and detailed drawing as shown in Figure 13. The mechanic parameters of the embankment are assumed based on Kanyama et al. [26]. The considered flood level with return period of 2 years is E.L. 84.89 m, as provided by the Third River Bureau of the Water Resources Administration of the Ministry of Economic Affairs. According to MOI [27], the short-period spectral acceleration coefficient of the site is 0.8; the short-period site amplification factor ( $F_a$ ) is 1.0; the short-period near-fault adjustment factor ( $N_A$ ) is 1.23 with the control fault of Chelungpu Fault. According to the above information, the horizontal peak ground acceleration (PGA) of this site is 0.3936 g. The moment magnitude ( $M_w$ ) of the design earthquake is 7.1.



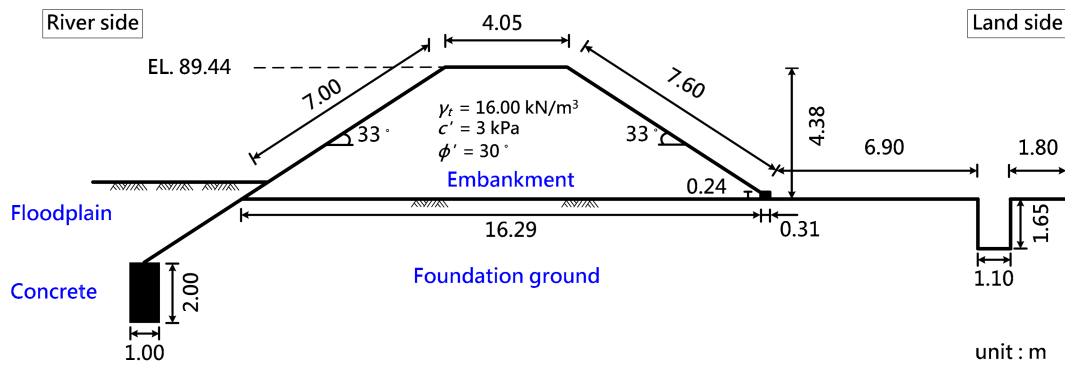














Figure 13. The geometry and material properties of the embankment.

Because there is no actual drilling data for the embankment, the drilling results of the adjacent National Highway No. 3 Expressway were used as the stratum profile on the site. The drilling data are shown in Table 5. The liquefaction potential of the site, as evaluated by the stress-based simplified HBF method, is also shown in Table 5. Please refer to Hwang et al. [18] for the detailed soil liquefaction evaluation procedure. It should be noted that if there are no reliable drilling results for reference, it is recommended that supplementary geotechnical drilling work be carried out to obtain reasonable geotechnical data.

Table 5. The information of the reference borehole.

Logging	USCS	Depth (m)	$\gamma_t$ (kN/m <sup>3</sup> )	SPT-N	FC (%)	Soil Liquefaction Evaluation		
						CSR	CRR	F <sub>L</sub>
	ML	0.8	18.25	2	56	—	—	3.00
	SM	2.7	18.44	7	29	0.29	0.18	0.61
	SM	3.7	18.44	7	29	0.34	0.16	0.47
	SM	4.9	19.33	13	20	0.37	0.25	0.69
	SM	6.0	19.72	4	17	0.39	0.11	0.29
	SM	6.7	19.91	19	30	0.39	0.46	1.18
	SM	8.3	19.91	16	30	0.40	0.28	0.70
	SM	11.0	21.19	32	30	—	—	3.00
	CL	13.3	20.40	16	75	—	—	3.00
	CL	14.0	20.40	27	75	—	—	3.00
	SM	17.0	21.19	28	30	0.34	0.45	1.33
	GM	19.0	22.00	100	—	—	—	3.00

Note: GWT = 1.54 m.

#### 4.2. Preliminary Seismic Evaluation

According to the field investigation, the embankment is filled with sandy material. The unit weight of the embankment was assumed to be  $16.0 \text{ kN/m}^3$ . The site is a multi-layer foundation site as shown in Table 5. After engineering judgment, the multi-layer foundation was simplified to one layer. The geotechnical parameters used the weighted average of multiple layers of soil above the depth of 8.3 m. The simplified stratum was regarded as sandy material, for which the unit weight is  $18.4 \text{ kN/m}^3$ , average SPT-N is 9.7, FC is 30%, and friction angle is  $28.9^\circ$ . Since the soil type of the simplified soil was sandy material, the soil type dependent coefficient of  $N_1$  derived from Figure 5 was 3.2. The standard factor of safety ( $F_{ss}$ ) was 1.66, which was calculated from the equation of  $N_1 \tan(\phi)$  mentioned in Section 3.1. Information on the ground material and geometry of the embankment in hand, the correction coefficients of  $\mu_1$  and  $\mu_2$  could be derived from Figure 4 and Table 2 and were 1.0 and 0.9, respectively; the static factor of safety ( $F_{S0}$ ) was 1.49 according to Equation (1).

Regarding the dynamic factor of safety ( $F_{Sd}$ ), in the case considering the earthquake-induced inertial force  $F_{Sd}(k_h)$ , the essential parameters of the horizontal seismic coefficient  $k_h$  and the reduction factor ( $\alpha$ ) were found to be  $\text{PGA}/2 = 0.197 \text{ g}$  and 0.49, respectively, by checking Figure 6 with the information on  $k_h$ . According to Equation (2), the  $F_{Sd}(k_h)$  can then be calculated as 0.73. In the case considering soil liquefaction  $F_{Sd}(\Delta u)$ , it can be seen in Table 5 that the depth above 8.3 m of the site, which is the range considered by the simplified stratum for preliminary seismic evaluation, consisted of many liquefied layers ( $F_L < 1.0$ ) subjected to the design earthquake, with a minimum  $F_L$  of 0.29. In comparison to Table 3, the reduction factor ( $\beta$ ) was 0.25. According to Equation (3), the  $F_{Sd}(\Delta u)$  could then be calculated as 0.37.

Information on  $F_{Sd}(k_h)$  and  $F_{Sd}(\Delta u)$  in hand, according to Table 4, the seismic safety classification was IV and the settlement of the embankment was  $>3.3 \text{ m}$ , which is  $>0.75$  times the height of the embankment.

#### 4.3. Detailed Seismic Evaluation (Static Softening Method, SSM)

In this study, the two-dimensional explicit finite difference code FLAC [24] was used to investigate the deformation and damage of the embankment caused by the liquefaction of the foundation soil under the condition of the target earthquake with the SSM. The analysis section of this study was located at the embankment on the side of Maoluo River. Please refer to Section 4.1 for the basic information and standard analysis section. Figure 14 shows the numerical analysis grid of the standard analysis section and the boundary condition. The number of grids is about 1900. The size of the grids near the embankment is relatively small to obtain more accurate analysis results. The ones close to the left and right boundaries are larger to save computational time for numerical analysis. The left and right boundaries of the model are set with roller condition that restrain the horizontal displacement satisfy the settlement and uplift phenomenon when the stratum is deformed; the bottom of the model is set with roller condition to restrain vertical displacement. The elevation of ground water tables on the left side boundary (river side) and right side boundary (land side) of the model are set according to the Q2 flood level elevation (E.L. 84.89 m) and the groundwater level observed from the drilling data (E.L. 84.09 m), respectively.

The soil parameters of the model are shown in Table 6. The focus of SSM of river embankment liquefaction is the weakening of liquefied soil parameters. For the consideration of the parameters of the liquefied soil layer, the liquefaction potential of the saturated sandy soil should be evaluated first by the stress-based simplified HBF method. The ones with  $F_L < 1.0$  were regarded as the soil that will undergo soil liquefaction during the earthquake, which is indicated in Table 6 and Figure 14.

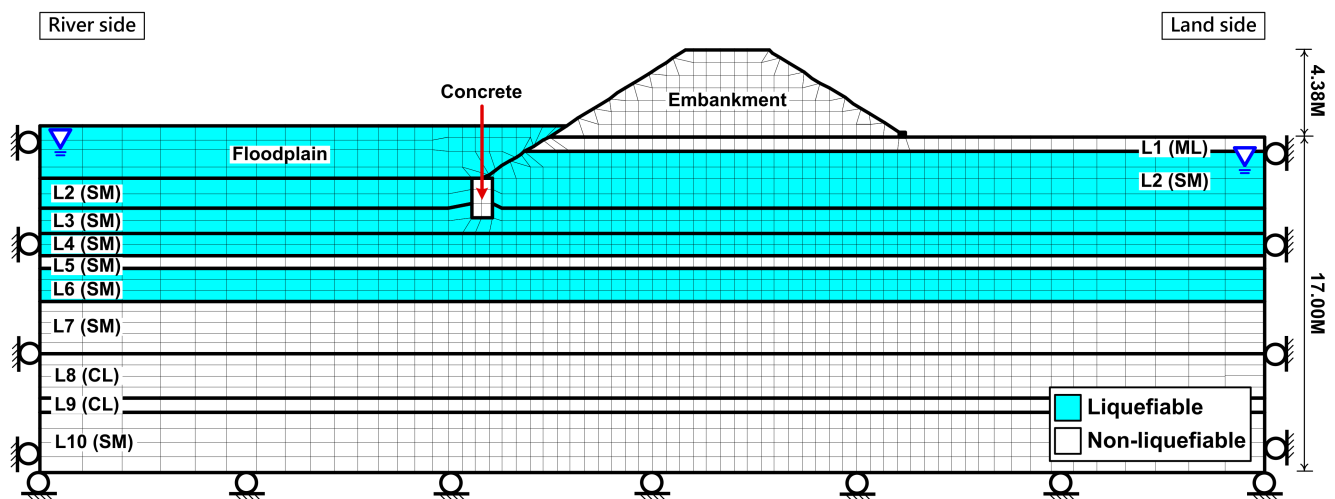


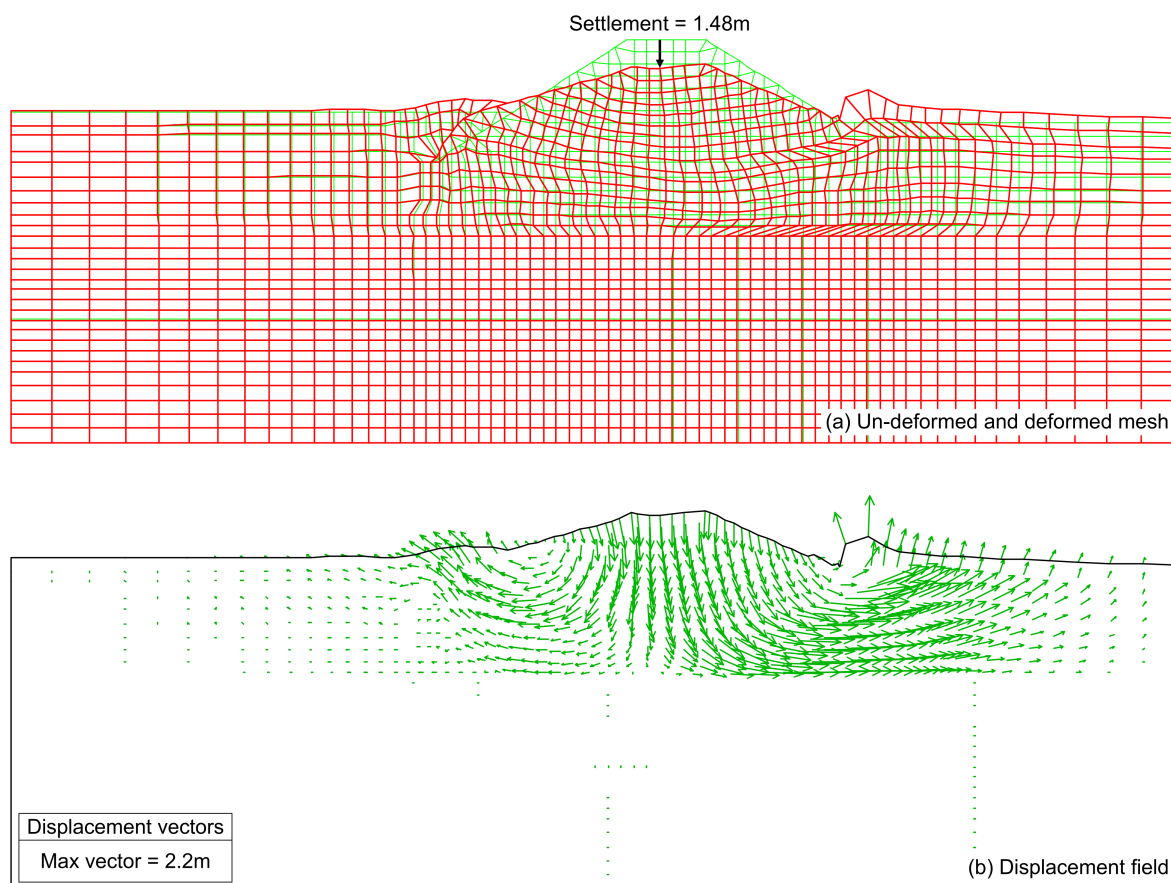
Figure 14. The numerical model of the embankment.

Table 6. The soil parameters of the numerical model.

Soil Layers	USCS	N-Value	$\gamma_t$ (kN/m <sup>3</sup> )	$c'$ (kPa)	$\phi'$ (deg)	G (MPa)	K (MPa)	Liq?
Embankment	SM	10	16.37	3.0	30.0	9.08	27.25	No
Floodplain	SM	10	19.35	1.0	29.1	9.08	27.25	Yes
L1	ML	2	18.60	23.5	0.0	1.75	8.18	No
L2	SM	7	18.81	0.0	26.8	6.36	19.08	Yes
L3	SM	13	19.75	0.0	31.1	11.81	35.43	Yes
L4	SM	4	20.10	0.0	23.9	3.63	10.90	Yes
L5	SM	19	20.28	0.0	34.5	17.26	51.78	No
L6	SM	16	20.28	0.0	32.9	14.53	43.60	Yes
L7	SM	32	21.56	0.0	40.3	29.07	87.20	No
L8	CL	16	20.80	94.2	0.0	13.17	654.00	No
L9	CL	27	20.80	158.9	0.0	22.22	1103.63	No
L10	SM	28	21.58	0.0	38.7	25.43	76.30	No

When performing numerical analysis, after the numerical mesh and boundary condition are established, the soil parameters shown in Table 6 were assigned in the corresponding soil layers, and the self-weight balance was then carried out to generate the initial stress. After the equilibration was complete, the numerical analysis model including the embankment and the foundation formation produced the initial stress conditions. Before the weakening analysis was carried out, the strength and elastic parameters of the liquefied soils were updated first. The undrained shear strain ( $S_u$ ) was obtained according to the empirical formula for the relationship between normalized residual shear strength ( $S_u / \sigma'_{v0}$ ) and clean sand equivalence of corrected SPT blow count ( $(N_1)_{60cs}$ ) suggested by Stark and Mesri [22] or Idriss and Boulanger [23]. For the elastic parameters of the liquefied soils, the Young's modulus (E) was obtained based on the empirical relationship of  $E / S_u = 300$ , and the Poisson ratio ( $\nu$ ) is assumed to be 0.49 to satisfy the undrained condition of the liquefied soils. Upon obtaining the E and  $\nu$ , the shear modulus and bulk modulus of the liquefied soil layer could be obtained based on the theory of elasticity. After updating the parameters of the liquefied soils in the program, the balance calculation was performed again by the program, and the deformation behavior of the embankment after the liquefaction of the foundation soil was observed.

While conducting the stress balance analysis after assigned the weakening parameters in the program, the settlement increment of the top of the embankment was monitored. The stress balance analysis stopped when the evaluated settlement has no significant increase, which meant that the stress state of the whole analysis model had become stable. Figure 15 shows the final numerical mesh and displacement field after assigning the lower relationship weakening parameters suggested by Stark and Mesri [22]. Other scenarios including the upper relationship weakening parameters suggested by Stark and Mesri [22] and lower relationship and upper relationship parameters suggested by Idriss and Boulanger [23] are not shown because their deformation patterns are similar to Figure 15. From the mesh before and after the weakening analysis, the settlement and deformation of the embankment caused the ground on both sides of the embankment toe to be squeezed and uplifted. The mesh deformation mainly occurred in the embankment and the liquefied layers below the embankment. The settlement figures of the embankment using the upper relationship and lower relationship weakening parameters suggested by Stark and Mesri [22] were 0.79 m and 1.48 m. The settlement figures of the embankment using the upper relationship and lower relationship weakening parameters suggested by Idriss and Boulanger [23] were 0.30 m and 1.00 m. According to Table 4, the seismic safety classification was I~II.



**Figure 15.** The SSM results of the embankment with the lower relationship weakening parameters suggested by Stark and Mesri [22].

#### 4.4. Detailed Seismic Evaluation (Dynamic Effective Stress Method, DESM)

In this study, the two-dimensional explicit finite-difference code FLAC [24] was also used to explore the deformation and damage of the embankment caused by the liquefaction of the foundation soil under the condition of the design earthquake by the DESM. The Itasca developed FLAC program can carry out dynamic analysis in the time domain for earthquake engineering problems. During the DESM, the acceleration duration input is assigned on the bottom boundary to simulate the loading of external earthquake forces.

Upon setting of boundary conditions that satisfy the field condition and the use of soil constitutive models such as the Finn model or PM4Sand model, the hysteretic damping effect and build-up of excess pore water pressure due to the cyclic loading can be reasonably simulated, and the acceleration, dynamic stress, displacement, and build-up of excess pore water pressure of each soil element can thus be obtained.

The DESM uses the same numerical mesh as the SSM. The process to yield initial condition (before earthquake) is also the same as the SSM. Before the simulation of DESM, the left and right boundaries need to be set to a synchronous motion state to simulate the uniform deformation of the free field. While conducting the DESM, the bottom of the model is the position to input the external force. During the dynamic analysis process, the acceleration or velocity of the base is controlled by the input external force during the analysis. In addition, it should be noted that when performing dynamic mechanical analysis, the size of the grids needs to be checked based on the input signal frequency. If the numerical grid size is too large, it will not be able to transmit high-frequency signals in the seismic duration. The grid size in this study is about 0.65 m. In the soil medium, the lowest shear wave velocity is about 140.7 m/s, so the highest frequency of the seismic input is 21.65 Hz according to the grid size suggested by Kuhlemeyer and Lysmer [28].

For the selection of the input motion, the 1999 Chi-Chi Earthquake records of TCU076 station shown in Figure 16 were adopted for a seed earthquake. While conducting the spectral matching in frequency domain, a seed (real) earthquake record should be given to provide the characteristic of waveform. In general, the seed earthquake is selected from the records of the seismic station near the site. The distance of the TCU076 station to the site is about 1.6 km, and the seismic characteristics of the recorded 1999 Chi-Chi Earthquake are close to the level of design earthquake of the national seismic design code, which is believed to be qualified to represent the seismic characteristic of the site. The selected earthquake records were then performed by the process of baseline correction, and the vector synthesis of the two horizontal acceleration durations (EW and NS) was conducted to yield the action direction perpendicular to the longitudinal axis of the embankment. Because the analysis grid could just reasonably reflect the seismic signal frequency of dynamic behavior below 21.65 Hz, the seismic record higher than 10 Hz was filtered in this study in order to avoid high-frequency seismic signals from interfering with the results of numerical analysis. After this, the spectral matching in frequency domain was carried out based on the response design spectrum suggested by MOI [27] and the seed earthquake after the adjustment of the action direction to obtain an artificial acceleration time history that was appropriate to site conditions. The normalized input (artificial earthquake) of the numerical model as well as the normalized seed earthquake is shown in Figure 17. As mentioned in Section 4.1, the horizontal peak ground acceleration (PGA) of this site is 0.3936 g. Note that the response of the outcrop motion occurs at a free surface at the site and it is about twice the upward wave-train motion. Therefore, the seismic input for the numerical model, which is the upward-propagating motion at the bottom boundary, needed to be computed by taking half the outcrop motion. Thus, the peak of the input was 0.197 g (PGA/2).

Referring to the basic information of the demonstration site, the simplified stratum soil parameters used for DESM are shown in Table 7. For sandy soils with liquefaction potential, this study used the PM4Sand model developed by UC Davis in the United States [25] in order to reasonably simulate the build-up of excess pore water pressure of liquefied soils during cyclic loading. The setting parameters were mainly obtained by using the SPT-N value and the dynamic strength curve. For the clay layers or the one above the ground water table, because the excess pore water pressure is not large, the Mohr–Coulomb model accompanied by FLAC built-in hysteretic damping was used in the analysis. To simulate the seepage during the dynamic analysis, the hydraulic conductivity of each layer was assigned based on the engineering experience.



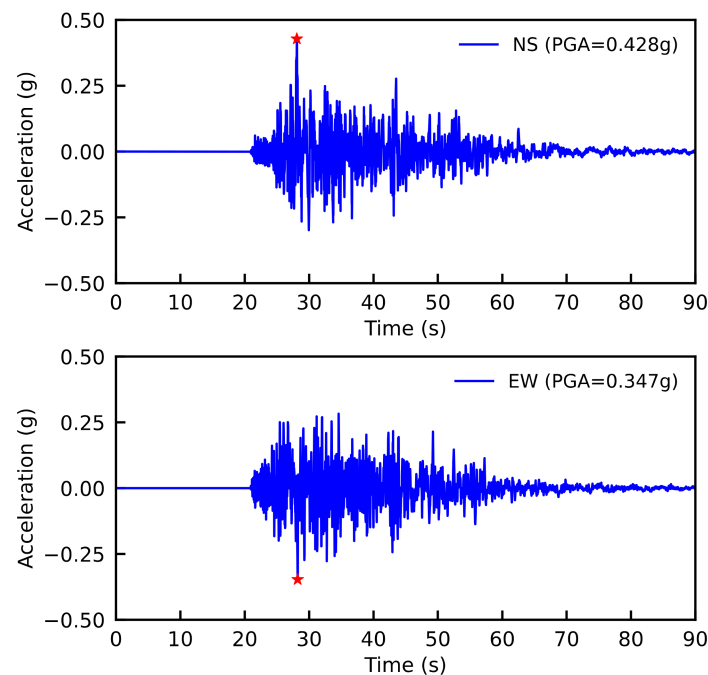


**Figure 16.** The 1999 Chi-Chi Earthquake acceleration histories recorded by TCU076 station.

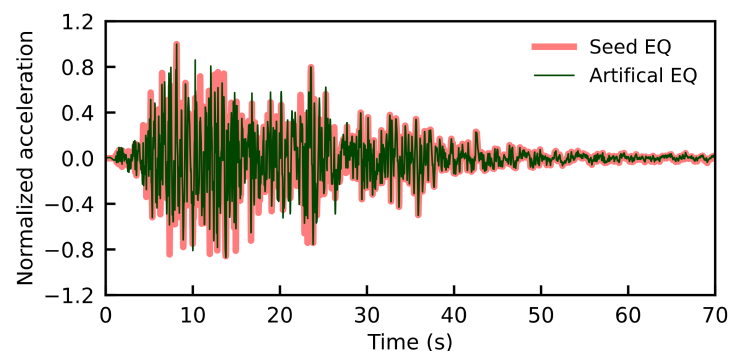


**Figure 17.** The normalized artificial earthquake and seed earthquake.

After the simulation of the initial state before the earthquake was completed, for which the procedure is the same as SSM, the soil constitutive models and the corresponding parameters shown in Table 7 were assigned and the seismic acceleration duration was then input from the bottom of the model. The  $G_o$  parameter in the PM4Sand model shown in Table 7 is calibrated based on SPT-N value according to the suggestion of PM4sand developers [25]. The contraction rate parameter ( $h_{po}$ ) was carefully calibrated by the triaxial cyclic resistance curve of the undisturbed Maoluo River sandy soil specimens retrieved for shallow depth soils [29]. Please refer to Figure 18 for the calibration result of  $h_{po}$ . For the non-liquefiable sandy soils with depth deeper than 10 m (L10), the 0.4 of  $h_{po}$  in PM4Sand was used due to the lack of reliable reference and their little influence on the analysis results.

The dynamic response of the model could then be captured during the earthquake by monitoring the acceleration, pore water pressure change duration, and stress and strain of each soil element at each time point. The dynamic deformation, residual deformation, and the liquefaction area could be thus observed.

**Table 7.** The soil parameters for dynamic effective stress method (DESM).

PM4Sand Model							
Soil Layers	USCS	$\gamma_t$ (kN/m <sup>3</sup> )	$D_r$	$\nu$	$G_o$	$h_{po}$	Hydraulic Conductivity, k (cm/s)
Floodplain	SM	19.35	0.69	0.35	738	0.2	$1.96 \times 10^{-3}$
L1	ML	18.60	0.33	0.40	447	0.2	$9.80 \times 10^{-5}$
L2	SM	18.81	0.55	0.35	614	0.2	$3.92 \times 10^{-3}$
L3	SM	19.75	0.67	0.35	770	0.2	$1.96 \times 10^{-3}$
L4	SM	20.10	0.35	0.35	473	0.2	$9.80 \times 10^{-3}$
L5	SM	20.28	0.78	0.35	917	0.2	$1.96 \times 10^{-3}$
L6	SM	20.28	0.69	0.35	825	0.2	$1.96 \times 10^{-3}$
L7	SM	21.56	0.92	0.35	1154	0.2	$9.80 \times 10^{-4}$
L10	SM	21.58	0.77	0.35	984	0.4	$1.96 \times 10^{-3}$
Mohr–Coulomb + hysteretic damping							
Soil layers	USCS	$\gamma_t$ (kN/m <sup>3</sup> )	$c'$ (kPa)	$\phi'$ (deg)	G (MPa)	K (MPa)	Hydraulic conductivity, k (cm/s)
Embankment	SM	16.37	3.0	30.0	53.7	161.2	$9.80 \times 10^{-4}$
L8	CL	20.80	94.2	0.0	95.4	4739.3	$9.80 \times 10^{-6}$
L9	CL	20.80	158.9	0.0	135.3	6717.5	$9.80 \times 10^{-6}$

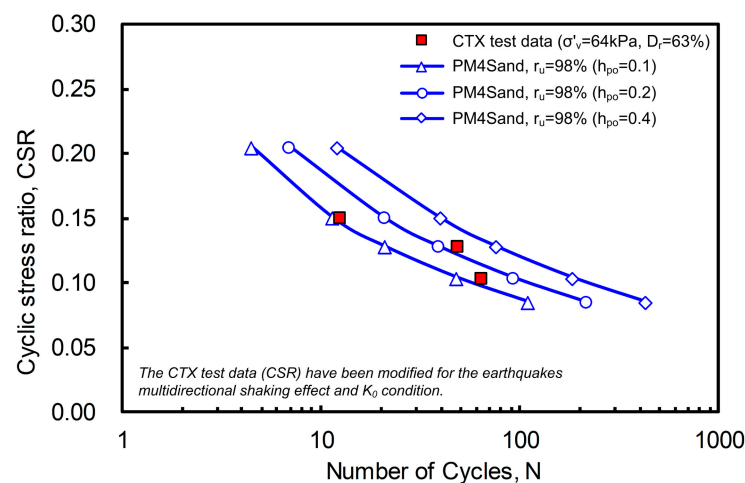


**Figure 18.** The calibration of  $h_{po}$  based on the dynamic triaxial test results.

Figure 19 shows the distribution of excess pore water pressure ratio ( $r_u = \Delta u / \sigma'_{v0}$ ) at earthquake time of 10 s. In the figure, the sand layer (L4) has reached a liquefied state ( $r_u \approx 1.0$ ). Figure 20 shows the excess pore water pressure ratio history of the central element of L4 layer during the earthquake. In the figure, the soil layer reached the initial liquefaction state when the earthquake time was at about 5.6 s, and the liquefaction state continued until the earthquake had lasted about 50 s. After 50 s, the excess pore water pressure gradually dissipated as the seismic wave acceleration amplitude decreased. From the change of the stress–strain curve and the stress path of the liquefied layer, it can be seen that with the liquefaction of the sand layer (L4) during the earthquake, the soil stiffness decreased and the slope of the stress–strain hysteresis circle became gentler, indicating that the soil began to soften as shown in Figure 21.

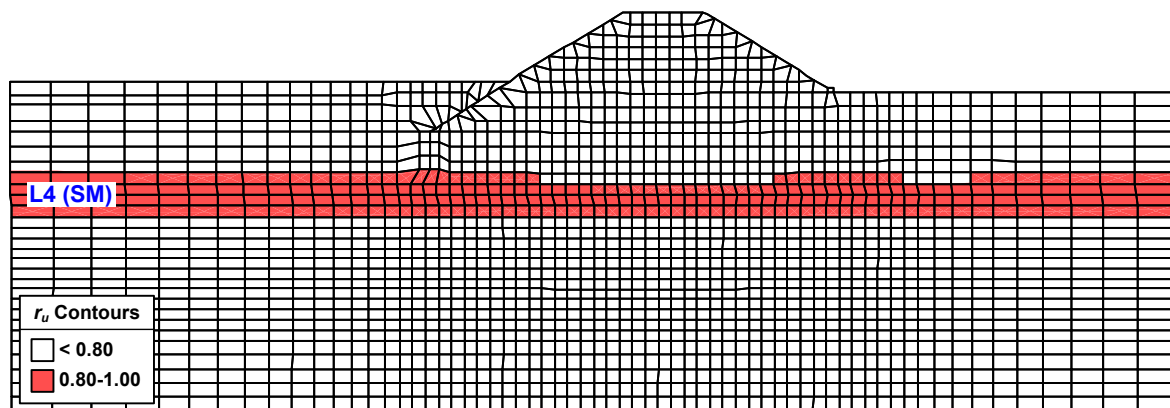


Figure 19. The distribution of EPWP ratio at earthquake time of 10 s.

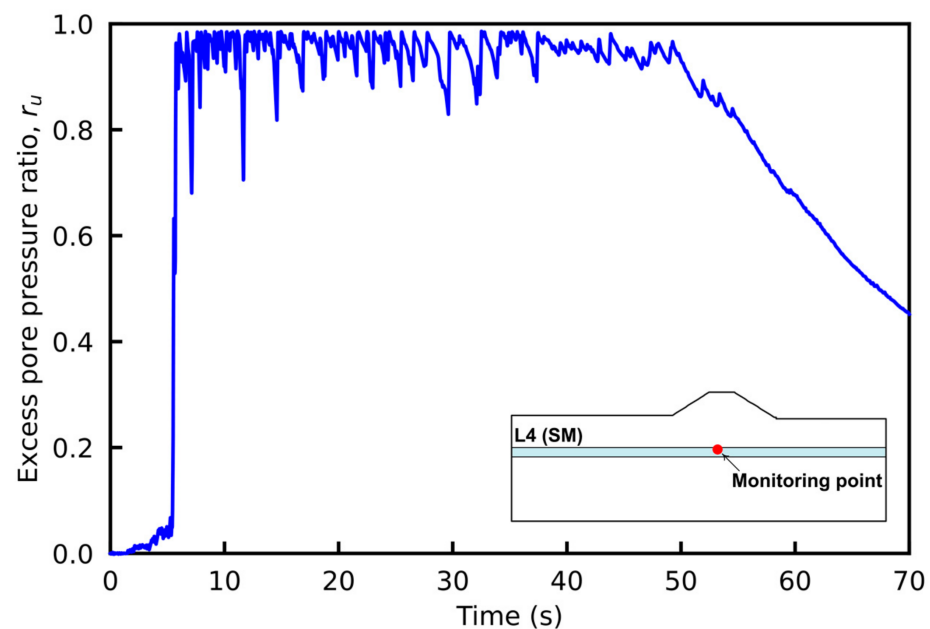
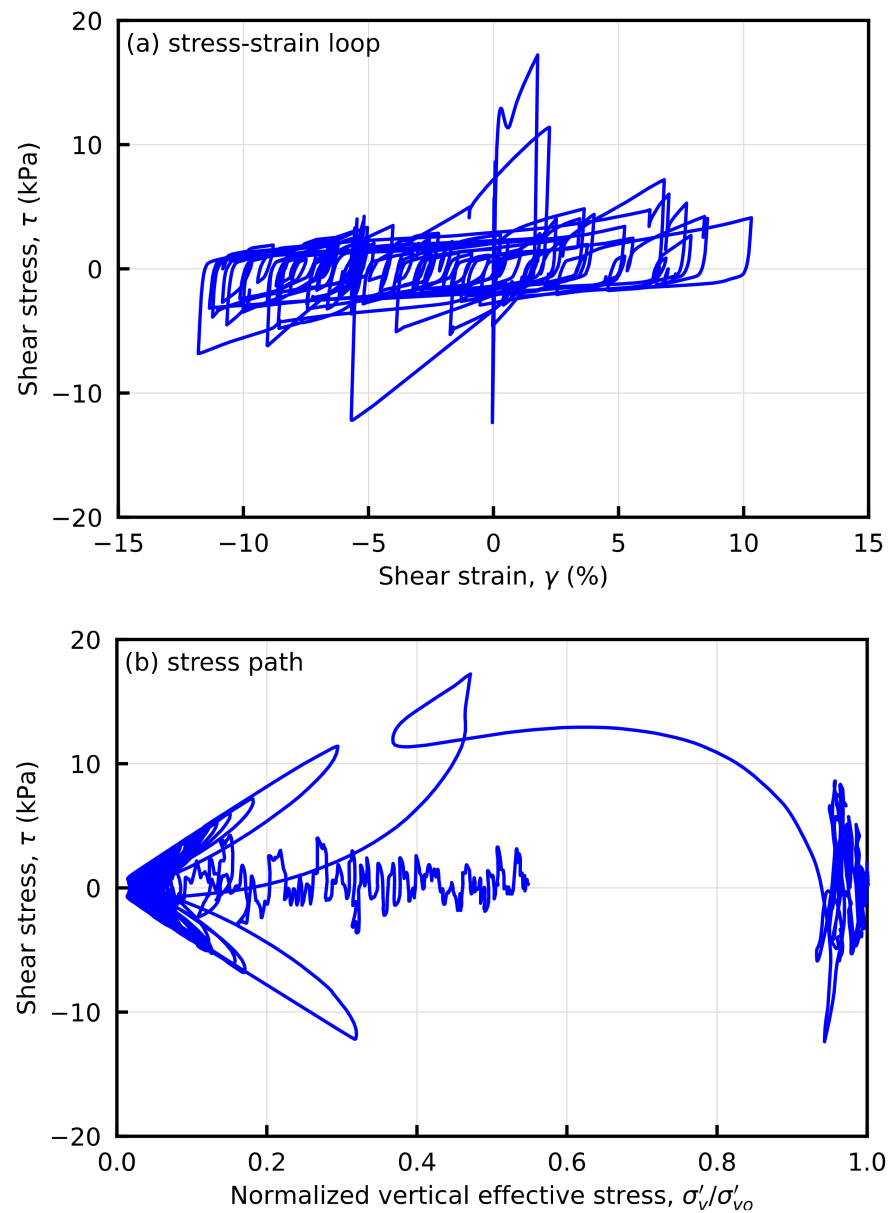
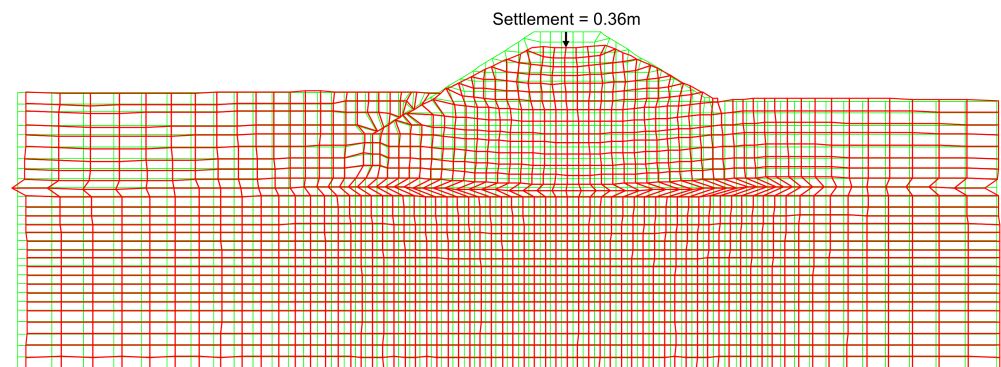


Figure 20. The EPWP ratio history at the central element of L4 layer during the earthquake.

Figure 22 shows the mesh deformation before and after the DESM. Figure 23 shows the displacement field at the end of the earthquake. As shown in the figures, the residual deformation of the embankment after seismic loading is different from that in the SSM. In the dynamic analysis, because the seismic wave was loaded horizontally, the overall model had obvious lateral displacement, and the embankment and its surrounding areas were plastically damaged due to the liquefaction of the foundation soil. The settlement of the embankment top obtained by the DESM is 0.36 m, and the horizontal displacement is 0.21 m. The settlement history of the embankment top is shown in Figure 24. It can be obviously found that the settlement of the embankment largely increased when the L4 layer occurred with soil liquefaction at earthquake time of 5.6 s. The dramatic increase of the settlement lasted until the earthquake time of 10 s and the accumulation rate became gentler thereafter.



**Figure 21.** Dynamic response at the central element of L4 layer during the earthquake. (a) stress-strain loop; (b) stress path.



**Figure 22.** The numeral mesh before and after earthquake.

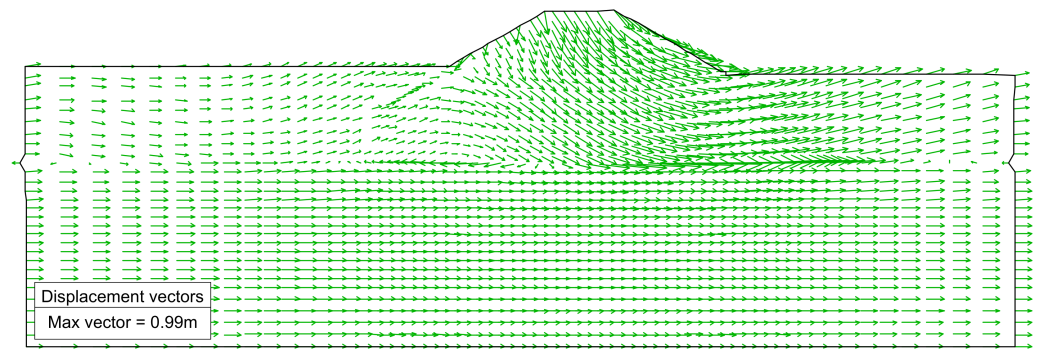


**Figure 23.** The displacement field after earthquake.

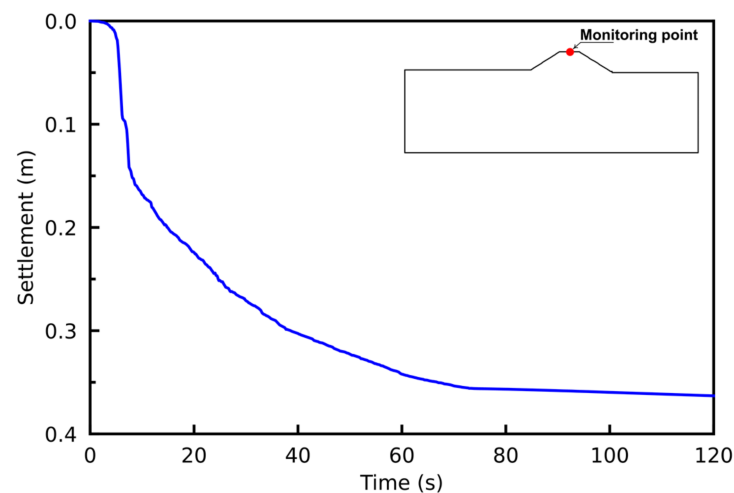


**Figure 24.** The settlement history at the top of the embankment.

#### 4.5. Discussion

In this research, the settlement of the river embankment after being liquefied by an earthquake was evaluated by a preliminary seismic evaluation and detailed seismic evaluation including the SSM and DESM. Please refer to Table 8 for the seismic classification results of all analyses. According to the analysis results, the preliminary seismic evaluation is based on the graphs, tables and empirical formulas and is the most conservative. In the analysis results of the SSM, the lower relationship of the empirical parameters softening formula suggested by Stark and Mesri [22] was the most conservative to evaluate the post-seismic settlement of the embankment, where the settlement of the embankment top reached 1.48 m; the one using the lower relationship of the empirical formula suggested by Idriss and Boulanger [23] was second, where the analyzed settlement was up to 1.0 m; the one using the upper relationship of the empirical formula suggested by Stark and Mesri [22] was third, where the analyzed settlement was about 0.79 m; the one with the use of the upper relationship of the empirical formula suggested by Idriss and Boulanger [23] was the least conservative, where the estimated settlement of the embankment top was 0.3 m, which was similar to the DESM result. Among the analysis methods of river embankment subjected to soil liquefaction, DESM stress is the most complete analysis method. Therefore, when evaluating the post-seismic settlement of river embankments, the results of DESM should be more accurate and representative. According to the results of the seismic evaluation, it can be roughly summarized that the analysis results of the preliminary seismic evaluation are the most conservative, followed by the SSM of detailed seismic evaluation, and the settlement of the embankment top obtained by the DESM of detailed seismic evaluation is the smallest.



**Table 8.** Seismic evaluation results of all analyses.

Item	Preliminary Seismic Evaluation	Detailed Seismic Evaluation				
		SSM				DESM
		Stark & Mesri [22]		Idriss & Boulanger [23]		
		Upper Relation.	Lower Relation.	Upper Relation.	Lower Relation.	
Settlement (m)	3.29	0.79	1.48	0.30	1.00	0.36
Settlement ratio <sup>a</sup> (%)	>75.0	18.0	33.7	6.9	22.8	8.0
Seismic safety classification	IV	I	II	I	I	I

<sup>a</sup> Settlement ratio = settlement/the height of the embankment (4.38 m).

## 5. Concluding Remarks

This study proposes a practical seismic assessment process, supplemented by demonstration cases to illustrate the analytical details of various assessments. The research results are believed to be helpful for promoting the overall inspection of the seismic performance of domestic river embankments in the future. According to the research results, there are some findings and suggestions listed as below:

1. Among the analyses, the preliminary evaluation is the simplest and conservative, so it is suitable for the preliminary screening of river embankments without safety concerns. The SSM can basically capture the deformation patterns of embankments located above liquefiable ground. However, the selection of parameters for the SSM has a great influence on the results. When a practical engineer conducts the SSM, the site characteristics of the analysis case should be carefully considered, and the appropriate empirical formula for the reduction of soil parameters can thus be selected. For an embankment of high importance, it is recommended to carry out DESM to reasonably estimate the settlement of the embankment subjected to the earthquake.
2. In this evaluation process, the embankments with no safety concerns are initially screened out through simple screening criteria, so that the entirety of evaluation work can be more efficient. The proposed preliminary seismic evaluation only needs to use simple basic data; with the help of charts, tables and formulas, a relatively conservative earthquake resistance assessment of river embankments can be carried out. For the embankments with high safety concerns and high importance in the preliminary evaluation results, it is suggested that a detailed seismic evaluation be carried out; the SSM or DESM should be carried out using the FEM/FDM program to obtain a reasonable seismic response of the embankment.
3. River embankments are important flood prevention facilities. It is necessary to start planning for seismic safety assessment and classification for the river embankments that are of high importance (metropolitan areas) and are located in the areas with severe liquefaction potential. For seismic capacity less than the requirements, it is recommended that the administration quickly improve its earthquake resistance and avoid the risk of secondary disasters caused by post-earthquake floods. For the embankments of major rivers, the administration should conduct a comprehensive preliminary seismic evaluation to identify the sections with damage potential after the shaking of the earthquake, and carry out detailed earthquake resistance evaluation work for the reference of subsequent earthquake resistance reinforcement operations.
4. It is suggested that the preliminary screening work be carried out by competent personnel of the property management unit (such as the River Administration). The preliminary seismic evaluation in the earthquake resistance assessment process should be handled by professionals with a background in geotechnical engineering. For detailed seismic evaluation with high technical difficulty and the need to cooperate

with numerical analysis, it is recommended to entrust a professional consulting company to handle it.

**Author Contributions:** Formal analysis, K.-Y.C.; Methodology, C.-C.L.; Project administration, C.-C.L., Y.-T.C. and Y.-H.H.; Software, C.-C.L. and K.-Y.C.; Supervision, C.-C.L. and Y.-T.C.; Writing—original draft, C.-C.L.; Writing—review & editing, C.-C.L. and K.-Y.C. All authors have read and agreed to the published version of the manuscript.

**Funding:** The APC was funded by the Water Resources Planning Institute, Water Resources Agency, Ministry of Economic Affairs through Contract No. 110-J-14-02-2-003-009.

**Acknowledgments:** The authors wish to acknowledge the financial support provided by the Water Resources Planning Institute, Water Resources Agency, and Ministry of Economic Affairs. The authors also wish to acknowledge the assistance of Jin-Hung Hwang in reviewing a draft of this paper.

**Conflicts of Interest:** The authors declare no conflict of interest.

## References

- Public Construction Commission. *Rapid Diagnosis and Reinforcement Strategy for Port and River Embankments after Earthquake*; Report No. 106; Public Construction Commission: Taipei, Taiwan, 2000. (In Chinese)
- River Embankment Earthquake-Resistant Measures Emergency Review Committee. *Report (Draft) on How to Proceed with Future Earthquake Resistance Measures for River Embankments Based on the Great East Japan Earthquake*; River Embankment Earthquake-Resistant Measures Emergency Review Committee: Tokyo, Japan, 2011. (In Japanese)
- Sasaki, Y.; Towhata, I.; Miyamoto, K.; Shirato, M.; Narita, A.; Sasaki, T.; Sako, S. Reconnaissance report on damage in and around river levees caused by the 2011 off the Pacific coast of Tohoku earthquake. *Soils Found.* **2012**, *52*, 1016–1032. [[CrossRef](#)]
- Chiaradonna, A.; Tropeano, G.; d’Onofrio, A.; Silvestri, F. Interpreting the deformation phenomena of a levee damaged during the 2012 Emilia Earthquake. *Soil Dyn. Earthq. Eng.* **2019**, *124*, 389–398. [[CrossRef](#)]
- Tsai, C.C.; Hsu, S.Y.; Wang, K.L.; Yang, H.C.; Chang, W.K.; Chen, C.H.; Hwang, Y.W. Geotechnical reconnaissance of the 2016 ML6.6 Meinong Earthquake in Taiwan. *J. Earth. Eng.* **2017**, *22*, 1710–1736. [[CrossRef](#)]
- Kramer, S.L. *Geotechnical Earthquake Engineering*; Prentice Hall: Upper Saddle River, NJ, USA, 1996.
- Athanasopoulos-Zekkos, A.; Saadi, M. Ground motion selection for liquefaction evaluation analysis of earthen levees. *Earth. Spectra* **2012**, *28*, 1331–1351. [[CrossRef](#)]
- Perlea, V.; Chowdhury, K.; Perlea, M.; Hu, G. Selection of Most Appropriate Procedures for Seismic Evaluation of Levees Based on Case Histories. In Proceedings of the International Conference on Case Histories in Geotechnical Engineering, Chicago, IL, USA, 29 April–4 May 2013; Volume 79.
- Athanasopoulos-Zekkos, A.; Seed, R.B. Simplified methodology for consideration of 2D dynamic response of levees in liquefaction triggering evaluation. *J. Geotech. Geoenviron. Eng.* **2013**, *139*, 1911–1922. [[CrossRef](#)]
- Okamura, M.; Hayashi, S. *Damage to River Levees by the 2011 Off the Pacific Coast Tohoku Earthquake and Prediction of Liquefaction in Levees*; Geotechnics for Catastrophic Flooding Events, Taylor & Francis Group: London, UK, 2015; pp. 57–67, ISBN 978-1-138-02709-1.
- Athanasopoulos-Zekkos, A.; Pence, H.; Lobbstaël, A. Ground motion selection for seismic slope displacement evaluation analysis of earthen levees. *Earthq. Spectra* **2016**, *32*, 217–237. [[CrossRef](#)]
- Gobbi, S.; Lopez-Caballero, F.; Forcellini, D. Numerical analysis of soil liquefaction induced failure of embankments. In Proceedings of the 6th International Conference on Computational Methods in Structural Dynamics and Earthquake Engineering Methods in Structural Dynamics and Earthquake Engineering, Rhodes Island, Greece, 15–17 June 2017. [[CrossRef](#)]
- Chiaradonna, A.; Flora, A.; d’Onofrio, A.; Bilotta, E. A pore water pressure model calibration based on in-situ test results. *Soils Found.* **2020**, *60*, 327–341. [[CrossRef](#)]
- Chiaradonna, A.; Ziotopoulou, K.; Carey, T.J.; DeJong, J.T.; Boulanger, R.W. Dynamic Behavior of Uniform Clean Sands: Evaluation of Constitutive Model Calibration Protocols in the Element- and the System-Level Scale. In Proceedings of the Geo-Congress 2022, Charlotte, NC, USA, 20–23 March 2022.
- Water and Disaster Management Bureau, Ministry of Land, Infrastructure, Transport and Tourism. *Seismic Inspection Manual for River Embankments*; Water and Disaster Management Bureau, Ministry of Land, Infrastructure, Transport and Tourism: Tokyo, Japan, 2016. (In Japanese)
- Ministry of Forests, Lands, and Natural Resource Operations—Flood Safety Section. *Seismic Design Guidelines for Dikes*, 1st ed.; Ministry of Forests, Lands, and Natural Resource Operations—Flood Safety Section: Victoria, British Columbia, Canada, 2011.
- Ministry of Forests, Lands, and Natural Resource Operations—Flood Safety Section. *Seismic Design Guidelines for Dikes*, 2nd ed.; Ministry of Forests, Lands, and Natural Resource Operations—Flood Safety Section: Victoria, British Columbia, Canada, 2014.
- Hwang, J.H.; Khoshnevisan, S.; Juang, C.H.; Lu, C.C. Soil liquefaction potential evaluation—An update of the HBF method focusing on research and practice in Taiwan. *Eng. Geol.* **2021**, *280*, 105926. [[CrossRef](#)]

19. Youd, T.L.; Idriss, I.M.; Andrus, R.D.; Arango, I.; Castro, G.; Christian, J.T.; Dobry, R.; Liam, F.W.D.; Harder, L.F., Jr.; Hynes, M.E.; et al. Liquefaction resistance of soils: Summary report from the 1996 NCEER and 1998 NCEER/NSF workshops on evaluation of liquefaction resistance of soils. *J. Geotech. Geoenviron. Eng. ASCE* **2001**, *127*, 297–313. [[CrossRef](#)]
20. Japan Road Association (JRA). *Design Specifications for Highway Bridges, Part V Seismic Design*; Japan Road Association (JRA): Tokyo, Japan, 1996. (In Japanese)
21. Architectural Institute of Japan (AIJ). *Recommendations for Design of Building Foundations*; Architectural Institute of Japan (AIJ): Tokyo, Japan, 2001. (In Japanese)
22. Stark, T.D.; Mesri, G. Undrained Shear Strength of Sands for Stability Analysis. *J. Geotech. Eng. Div. ASCE* **1992**, *118*, 1727–1747. [[CrossRef](#)]
23. Idriss, I.M.; Boulanger, R.W. *Soil Liquefaction during Earthquakes*; EERI Monograph MNO-12; Earthquake Engineering Research Institute: Oakland, CA, USA, 2008.
24. Itasca. *FLAC: Fast Lagrangian Analysis of Continua*; Itasca Consulting Group Inc.: Minneapolis, MN, USA, 2011.
25. Boulanger, R.W.; Ziotopoulou, K. *PM4Sand (Version 3.1): A Sand Plasticity Model for Earthquake Engineering Applications, Technical Report No. UCD/CGM-17/01*; Center for Geotechnical Modeling, Department of Civil and Environmental Engineering, University of California: Davis, CA, USA, 2017.
26. Kanyama, M.; Horii, K.; Kojima, K. *Seismic Performance of Embankment Seismic Design*; Railway Technical Research Institute: Tokyo, Japan, 1999; Volume 13. (In Japanese)
27. Construction and Planning Agency, MOI. *Seismic Design Specifications and Commentary of Buildings*; Construction and Planning Agency, MOI: Taipei, Taiwan, 2011. (In Chinese)
28. Kuhlemeyer, R.L.; Lysmer, J. Finite element method accuracy for wave propagation problem. *J. Soil Mech. Found. Div. ASCE* **1973**, *99*, 421–427. [[CrossRef](#)]
29. Hwang, J.H.; Chang, C.T.; Chou, K.T.; Yu, M.S.; Jean, W.Y.; Yang, C.W.; Fang, J.S.; Tseng, L.S.; Wang, J.S.; Li, H.I. *A Study on the Local Applicability of Liquefaction Assessment Methods Based on the Chi-Chi Earthquake Liquefaction Case*; National Highway New Construction Bureau of Taiwan District, Ministry of Communications: Taipei, Taiwan, 2005. (In Chinese)